LAWRENCE
LIVERMORE
NATIONAL
LABORATORY

UCRL-CONF-230784

Full System Model of Magnetron Sputter Chamber - Proof-of-Principle Study

C. Walton, G. Gilmer, L. Zepeda-Ruiz, A. Wemhoff, T. Barbee

May 8, 2007

Materials Research Society Spring 2007
San Francisco, CA, United States
April 9, 2007 through April 13, 2007

Full System Model of Magnetron Sputter Chamber – Proof-of-Principle Study

Chris Walton*, George Gilmer, Luis Zepeda-Ruiz**, Aaron Wemhoff***, and Troy Barbee, Jr.***

***Nanolaminate Materials Program, Nonproliferation, Homeland, and International Security Directorate**

****Chemistry, Materials and Life Sciences Directorate**

***** Engineering Directorate**

Lawrence Livermore National Laboratory

This work was performed under the auspices of the U.S. Department of Energy by University of California Lawrence Livermore National Laboratory under contract No. W-7405-Eng-48.

ABSTRACT

The lack of detailed knowledge of internal process conditions remains a key challenge in magnetron sputtering, both for chamber design and for process development. Fundamental information such as the pressure and temperature distribution of the sputter gas, and the energies and arrival angles of the sputtered atoms and other energetic species is often missing, or is only estimated from general formulas. However, open-source or low-cost tools are available for modeling most steps of the sputter process, which can give more accurate and complete data than textbook estimates, using only desktop computations.

To get a better understanding of magnetron sputtering, we have collected existing models for the 5 major process steps: the input and distribution of the neutral background gas using Direct Simulation Monte Carlo (DSMC), dynamics of the plasma using Particle In Cell-Monte Carlo Collision (PIC-MCC), impact of ions on the target using molecular dynamics (MD), transport of sputtered atoms to the substrate using DSMC, and growth of the film using hybrid Kinetic Monte Carlo (KMC) and MD methods. Models have been tested against experimental measurements. For example, gas rarefaction as observed by Rossnagel and others has been reproduced, and it is associated with a local pressure increase of ~50% which may strongly influence film properties such as stress. Results on energies and arrival angles of sputtered atoms and reflected gas neutrals are applied to the Kinetic Monte Carlo simulation of film growth. Model results and applications to growth of dense Cu and Be films are presented.

INTRODUCTION

An accurate model of magnetron deposition systems is of great interest for process improvement and chamber design. For example, it is well known that film stress depends sensitively on the energies and the range of angles of incidence of the sputtered atoms. But it is not simple to calculate the effect of a process change (*e.g.* changing pressure or target-substrate distance) on these angles and energies. Precision control of stress therefore depends on empirical testing, which is generally expensive.

Many groups have modeled parts of the process.[1-6] Multiscale physics models based on continuum fluid mechanics exist, but do not include gas rarefaction, are likely to be inaccurate at low sputter pressures, and to have difficulty with gas mixtures.[7, 8] Kools[9] proposed that existing models of the different process steps could be used together to model an entire system, including neutral gas transport, plasma transport, sputter, and film growth. Miyagawa *et al*. have published some description of such a comprehensive model[10] but there appears to be little published data on its use. Because of internal interest at LLNL in precision microstructure and stress control, an effort was begun to model all the process steps with existing open-source or inexpensive codes, as suggested by Kools, for low-pressure (0.1-5mTorr) conditions.

STRUCTURE OF MODEL

The model components are Direct Simulation Monte Carlo (DSMC) for transport of neutral particles (Ar background gas and sputtered atoms), Particle-In-Cell (PIC) for plasma transport, Molecular Dynamics (MD) for sputter at the target, and Kinetic Monte Carlo (KMC) for film growth. Our PIC plasma model is not yet ready to give input to the other steps, so at this

stage it is replaced by a generic plasma assumption that all ions hit the target at normal incidence with the full sputter voltage (400eV). The data flow is shown in Fig. 1.

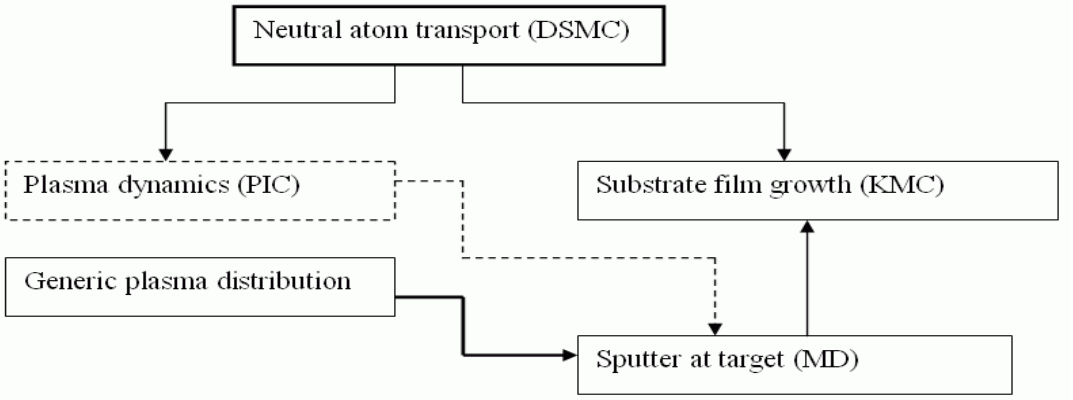

Figure 1. Model data flow. Heavy lines indicate that full coupling of models is in place; light lines indicate both models are running but simple cases are used for coupling for now; dotted lines indicate the coupling is possible but not yet implemented.

RESULTS

Transport of neutrals - DSMC

In magnetron sputtering, it is well known that the energetic sputtered atoms collide with the background gas atoms, heating them significantly if the current density is high. This heating causes a rarefaction of the gas, which was reported experimentally by Rossnagel[11] from measurements with a pressure probe tube. For high current density, this rarefaction can be as much as a ~85% reduction of the background gas density. The DSMC method is expected to fully include this effect because it contains an accurate simulation of the momentum transfer for collisions of all species with each other and with the walls.

To validate the use of DSMC for this application we have simulated the chamber used by Rossnagel in the work cited above. This chamber was a cylinder of diameter 60cm and height 24cm, with a 6-inch diameter circular magnetron mounted in the center of the cylinder's base. We used the 2D DSMC code DS2V, (version 3.7.03) published by G. A. Bird,[12, 13] with axial symmetry. The sputtered atoms were introduced using a range of narrow slits to express the angular end energy dependence of the sputtered flux. The case simulated has a current of 4A at a nominal chamber pressure of 1Pa of Ar, and a Cu target. The angle and energy distributions of atoms leaving the target were calculated with the Kalypso code by Karolewski.[14]

Results for pressure and temperature vs. position are shown in Fig. 2. The DSMC code models neutral Ar and Cu atoms only, and does not include magnetic or electric fields or any plasma effects. The fine features on the color maps are caused by the discrete sampling of energies and angles – these are "Mach disks" for the jets of Cu atoms from the slits. The sputter gas is heated to an average temperature of ~1000K in the hottest region on the gun axis. It also shows a pressure increase of 40-50% in the same region.

It has been assumed by most investigators of similar systems that the pressure is uniform throughout the chamber. While this is true in familiar atmospheric-pressure conditions where gases are under continuum flow, at low-pressure conditions (transition flow or molecular flow, or Knudsen number Kn > 0.01) it is possible to have a substantial pressure gradient at steady

state. This is true because when the mean free path is long the momentum transfer that would equalize pressure is slowed. This phenomenon is responsible for thermal transpiration in tubes but also occurs in open volumes. It is well summarized by Siu[15] as the statement that "temperature gradients induce pressure gradients".

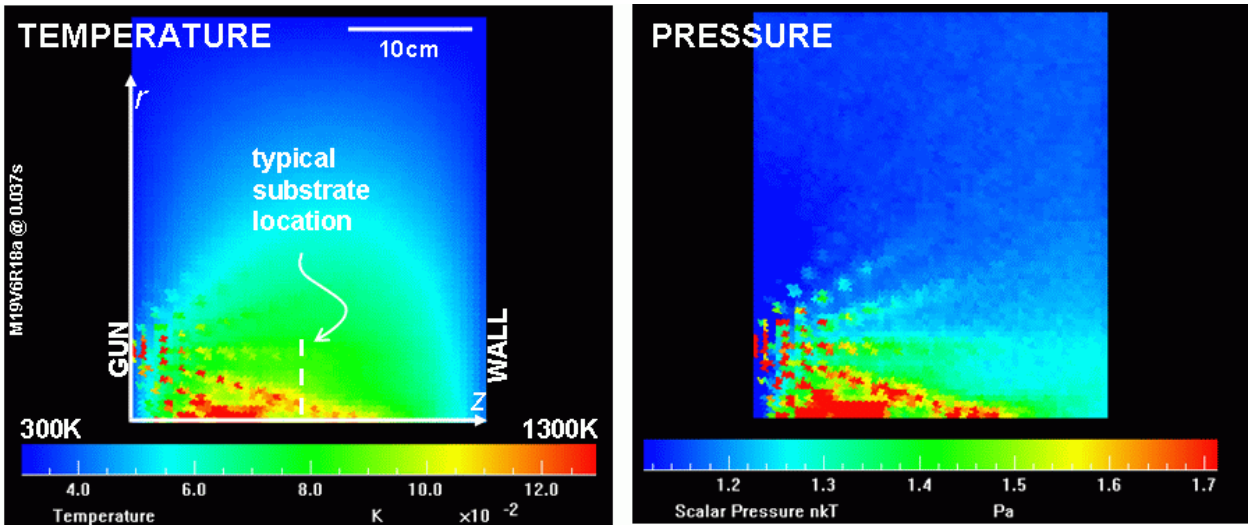

Figure 2. Axial DSMC simulation of pressure and temperature in chamber used by Rossnagel.[11] Region shown is a half-plane from axis of chamber (r = 0) to chamber wall (r = 30cm).

To test these results we did similar calculations of Rossnagel's chamber with a probe tube included. Including the tube is necessary to compare to his results because of strong thermal transpiration effects in the tube – the pressure measured at the cold end (gauge end) of the tube is not the same as the system pressure at the active end. Pressure at the cold end of the tube was compared to Rossnagel's experimental results (Fig. 3 in his paper) for pressure vs distance from the target (sputtering Cu with Ar at I = 4A) at system pressures of 1Pa and 4Pa. The agreement is reasonable (10-40% error) but further work is needed in validation.

Similar simulations were performed for the chamber used for deposition of Be films on spheres. This chamber is a cylinder 45cm in diameter with a 5cm diameter magnetron on one base, mounted off-center about 10cm from the wall. Rough angle distributions of Be atoms arriving at the substrate were used as input for growth simulations. A uniform energy of 4eV was used for the Be atoms.

Transport of plasma - OOPIC

For plasma simulation we have used the OOPIC Pro package (Tech-X Corp., Boulder, CO), which is based on the XOOPIC code developed at the University of California, Berkeley.[16] The DC magnetic field was sampled from an experimental distribution published by Bohlmark[17] and the simulation was run for an axial domain of 8cm radius and 15cm target-substrate distance (z) with an initial plasma near the target of $10^{15}m^{-3}$ and a target bias of -100V relative to the grounded walls. The simulation does not yet show a stable plasma. The source of this problem may be a number of factors, including some remaining divergence in the magnetic field from

sampling, which will be resolved with a consistency check on the field with a Laplace equation solver. Because of the early stage of this simulation we will not present detailed results.

Film Growth and Microstructure – MD and KMC

The Kinetic Monte Carlo (KMC) simulations were performed using ADEPT, a three-dimensional lattice MC model.[18] In the Be simulations, an hcp lattice is chosen for the sites where atoms of the crystal are allowed to reside. Polycrystalline growth is modeled by assuming all grains have the basal plane texture, and assigning an in-plane orientation randomly to each new island that is nucleated. New adatoms attaching to an existing island are assumed to maintain the same in-plane orientation as the island, unless the adatom attaches to more than one island. In that case, the atom takes on the orientation that gives it the lowest energy. The model includes ballistic deposition from the sputter target with realistic angular distributions, binding energies, and surface diffusion. The angular distribution for the impinging atoms corresponds to a collimated beam produced by a target that subtends a small solid angle. A binary collision model simulates atomic displacements resulting from energetic impinging particles.[19] ADEPT has been developed in order to describe the growth of metal films deposited by sputter deposition. The general features of ADEPT have been presented before[1] and we sketch here only a background understanding here.

Molecular dynamics methods using a potential for Be were used to parameterize the ADEPT code with the diffusion rates, the energetics of the crystal sites, and the kinetic energies of the atoms sputtered from the target by argon ions. A Be empirical interatomic potential was developed by Lenosky[20] for use in this project, based on the modified embedded atom (MEAM) form. The total energy is expressed in terms of pair and three-body functions that contribute to the charge density at a site. All functions are represented as splines, and are fitted to first-principles data using a simulated-annealing methodology for force matching. The potential is also fitted to experimental and first-principles values for cohesive energies and elastic constants of various crystalline lattices, including fcc, bcc, and hcp. Molecular dynamics simulations of the sputtering of the Be target with 400eV argon atoms were performed. The angular and energy distributions of the sputtered atoms were obtained, providing initial values for the Be atoms emanating from the target and entering the argon plasma on the way to the substrate. Their transport to the substrate is accounted for in the DSMC simulation.

The simulations consist of a succession of deposition and surface diffusion events. Deposition often involved the displacements of near-surface atoms in the vicinity of the point where the impinging atom makes contact with an atom in the film. Spontaneous evaporation of atoms has been neglected because of the relatively large cohesive energy of the deposited film and substrate compared with thermal energies, although film atoms are ejected as a result of collisions with impinging Be atoms. The angular distribution for impinging atoms is taken from an approximation of the incoming angle distributions calculated by DSMC.

Simulation of an hcp Be deposit with the basal plane parallel to the substrate surface, (0001) texture, is shown in Fig. 3(a), and in (b) this is compared to fcc Cu with (111) texture. Deposition of Be was at a T = 290K, and of Cu at 254K, corresponding to identical temperatures relative to the melting points of the two metals. Differences between the two films are mainly attributable to the different lattice structures: only the basal plane has the close-packed 2d array of atoms in hcp, whereas four distinct (111) planes are present in the fcc lattice. The three (111) planes in addition to the texture orientation provide fast diffusion paths to fill voids below the

growth surface in the case of fcc, but there are no such fast diffusion paths for hcp growth besides (0001). For this reason, the trapping of voids is more frequent for hcp film growth under these circumstances, although the surface structure is rougher because of the tilted (111) facets. Fig. 3(c) shows the simulated Be film after further deposition, with coarsening of the grains occurring as taller grains overgrow some of their neighbors. Coarsening is inevitable, since grains can be cut off by their neighbors, but no new grains are nucleated. Once the substrate is covered, each new layer will assume the orientation of the layer below, since it serves as a template to order the arriving atoms. Impurities that form a monolayer or more on the growth surface could cause a new grain orientation to nucleate, since they would interfere with the potential energy surface of the layer below and its ability to orient the atoms of the next layer.

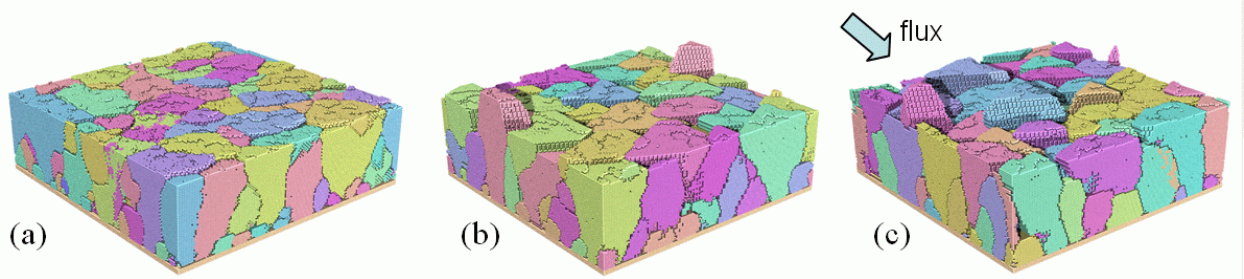

Figure 3. Computer generated graphics showing the film configurations of the ADEPT simulations for Be (a), Cu (b) and further growth on Be (c). The edge of the square substrate is 47 nm for the Be film, and 54 nm for Cu.

DISCUSSION

The Monte Carlo simulations show several important effects of the deposition conditions on film structure. First, as noted above, the angular distribution of the impinging atoms is reflected in the structure of the film, because of the limited mobility of atoms on the surface. The biased flux in Fig. 3 (c) results in increased roughness and in the number of voids; the preferential arrival of atoms from one side results in reduced flux to the valleys, leading to an instability in which the higher regions grow faster than the valleys. Eventually the valleys may be totally blocked, leading to void formation. Furthermore, the larger number of close-packed planes in the fcc lattice has an effect on roughness in the early stages of film growth, since atoms impinging on the substrate have a have high diffusivity paths with a vertical component to build up the height of the 3d islands, leading a rougher surface initially.

This work is at an early stage and much remains to be done. Nevertheless we believe there is valuable new understanding available through this approach because it includes Monte Carlo treatment of individual particles in order to get angle and energy distributions, because it includes local gas heating and rarefaction, and calculates the influence of these effects on film structure using a full three-dimensional model of thin film growth.

CONCLUSIONS

A model of most of the physics of a magnetron system can be constructed with existing codes for the various processes occurring. The codes used are capable of modeling realistic magnetron systems with computation times of hours or a few days. Preliminary results show coarsening and angle-dependent roughening for Cu films. Roughening was not predicted for Be up to a ~20nm film thickness. This appears to result from the lower symmetry of the hcp Be film

(only 1 dense-packed plane with high surface mobility). Comparison with experimental results on Be growth and the possible role of oxygen are active areas of investigation.

ACKNOWLEDGMENTS

The authors would like to thank Scott Wilks for helpful discussions in developing the plasma model, and Dan Rader and Michail Gallis for helpful criticism on use of DSMC.

REFERENCES

[1] G. M. Turner, Journal of Vacuum Science & Technology a-Vacuum Surfaces and Films **13**, 2161 (1995).
[2] S. D. Ekpe and S. K. Dew, Journal of Physics D (Applied Physics) **39**, 1413 (2006).
[3] S. Mahieu, G. Buyle, D. Depla, et al., Nuclear Instruments & Methods in Physics Research, Section B (Beam Interactions with Materials and Atoms) **243**, 313 (2006).
[4] H. M. Urbassek and D. Sibold, Journal of Vacuum Science & Technology A (Vacuum, Surfaces, and Films) **11**, 676 (1993).
[5] J. Q. Lu and M. J. Kushner, Journal of Applied Physics **87**, 7198 (2000).
[6] A. Kersch, W. Morokoff, and C. Werner, Journal of Applied Physics **75**, 2278 (1994).
[7] D. Zhang, P. J. Stout, and P. L. G. Ventzek, Journal of Vacuum Science & Technology A **21**, 265 (2003).
[8] A. V. Vasenkov, A. I. Fedoseyev, V. I. Kolobov, et al., in *2005 NSTI Nanotechnology Conference and Trade Show. NSTI Nanotech 2005. Anaheim, CA*, 2005).
[9] J. C. S. Kools, in *SVC - 47th Annual Technical Conference Proceedings* (Society of Vacuum Coaters, 2004), p. 31.
[10] Y. Miyagawa, M. Tanaka, H. Nakadate, et al., in *2000 International Conference on Ion Implantation Technology Proceedings. Ion Implantation Technology* (IEEE, Alpbach, Austria, 2000), p. 213.
[11] S. M. Rossnagel, Journal of Vacuum Science & Technology A-Vacuum Surfaces & Films **6**, 19 (1988).
[12] G. A. Bird, in *24th International Symposium on Rarefied Gas Dynamics RGD24. Bari, Italy. 10-16 July 2004*, 2005).
[13] G. A. Bird, Direct Simulation Monte Carlo Method:Visual Programs at GAB Consulting http://www.gab.com.au/).
[14] M. A. Karolewski, Nuclear Instruments & Methods in Physics Research Section B-Beam Interactions with Materials & Atoms **230**, 402 (2005).
[15] M. C. I. Siu, Journal of Vacuum Science and Technology **10**, 368 (1973).
[16] J. P. Verboncoeur, A. B. Langdon, and N. T. Gladd, Computer Physics Communications **87**, 199 (1995).
[17] J. Bohlmark, U. Helmersson, M. VanZeeland, et al., Plasma Sources Science and Technology, 654 (2004).
[18] H. Huang, G. H. Gilmer, and T. D. de la Rubia, Journal of Applied Physics **84**, 3636 (1998).
[19] J. Dalla Torre, G. H. Gilmer, D. L. Windt, et al., Journal of Applied Physics **94**, 263 (2003).
[20] L. A. Zepeda-Ruiz and T. J. Lenosky, unpublished.